Direct Comparison of Two Kinds of Linoleic Acid-docetaxel Derivatives: in Vitro Cytotoxicity and in Vivo Antitumor Activity

Lirui Jia
Shenyang Pharmaceutical University
Ying Liu
National Institute for the Control of Pharmaceutical and Biological Products: China National Institute for Food and Drug Control
Meng Li
Shenyang Pharmaceutical University
Yongjun Wang (i_maple@163.com)
Shenyang Pharmaceutical University
Zhonggui He
Shenyang Pharmaceutical University

Research Article

Keywords: Lipid-drug, Nanoassemblies, Anticancer efficacy, Cytotoxicity, Derivatives

Posted Date: March 11th, 2021

DOI: https://doi.org/10.21203/rs.3.rs-277092/v1

Version of Record: A version of this preprint was published at Drug Delivery and Translational Research on July 26th, 2021. See the published version at https://doi.org/10.1007/s13346-021-01010-8.

Abstract

Rational designed lipid-drug derivatives provide a favorable approach to improve the druggability of highly hydrophobic prototypes. It has been regarded as common sense that good cytotoxicity is the guarantee of superior anticancer efficacy for candidate derivatives screening. Here, we established two lipid-drug derivatives with different bridge bonds (ester bond and mono thioether bond) linking docetaxel and linoleic acid. The IC_{50} of DSL NPs (DTX-S-LA nanoparticles) and DL NPs (DTX-LA nanoparticles) were 4.02 and 209.6 ng/mL (DTX equivalent concentration), respectively. However, DL NPs unexpectedly showed stronger tumor inhibition abilities than DSL NPs. To explain the non-positive correlation between cytotoxicity and anticancer efficacy, more experiments were carried out in depth. Remarkably, the drug release studies in blood and PK study both suggested that the DL NPs were more stable to remain the structural integrity in circulation, which resulted in more accumulation in tumor sites. As verified by the bio-distribution study, DL NPs performed a superior target effect than DSL NPs in tumors. Our data indicated that the biological fates of so-called smart bond inserted derivatives *in vivo* are complicated, thus, simple cytotoxicity is not enough for derivatives screening, and the comprehensive understanding of both *in vitro* and *in vivo* behaviors is essential.

1. Introduction

Malignant tumor is a deadly threat to human health and life. At present, chemotherapy, supplemented by surgical and radiation treatment, is still the main treatment regimen for cancers [1–4]. Sadly, the clinical translation and usage of the vast majority of chemical substances have been largely limited due to its' fast elimination and hydrophobicity. Lipid-drug derivatives synthesized by conjugating hydrophobic chemotherapeutic drugs with fatty acid via various linkers have been widely studied to improve the druggability [5–7]. Fatty acid as adjuvant matrice not only produces cytotoxic agents though lipid peroxidation effect [8–11] but also renders double bonds and structural flexibility to facilitate the transformation of hydrophobic moieties into nanoassemblies. The conjugate nanoassemblies, with high drug loading, are potential treatment paradigms to break the bottleneck of prototype as reported [12–17].

For the massive drug candidates, tireless researches had been paid to find a simple favorable method for drug screening. 2D or 3D cultures of immortalized cancer cells have been widely used as primary *in vitro* tumor models in the high throughput screening of anticancer parent drugs owing to cytotoxicity is generally considered to have a positive relationship with the anticancer efficacy [18–21] However, is this cell-based drug screen still predictive for lipid-drug derivatives? Wang et al. [22] established six lipid-drug derivatives and conducted subsequent cytotoxicity assay on several cell lines. After screening by IC_{50}, the strongest cytotoxic lipid-drug derivative was chosen to perform the anticancer efficacy. But many critical issues which have been neglected lies in that the cytotoxic activity is structure-related and inhibition effect is affected by manifold causes [23, 24]. Some previous literature could support this view [20, 25, 26]. Steven et al. [27] synthesized nine lipid-paclitaxel derivatives with different linkers and anchors. He found that the efficacy correlated well with the PK profiles rather than cytotoxicity. The greatest antitumor response *in vivo* was not seen in the derivative with the lowest IC_{50}. Apart from this, our group previously

loaded disulfide bond and mono thioether bond insertions (DTX-ss-VE and DTX-s-VE) into liposomes. Though similar IC_{50}, these two liposomes possessed completely different inhibition effects *in vivo*. The anticancer efficacy of DTX-ss-VE loaded liposomes was comparable with DTX solutions, while no any inhibition effect was observed in DTX-s-VE loaded liposomes group [28].

The relationship between cytotoxicity and anticancer efficacy especially for derivatives is of great importance. Misuse of this relationship would bring about inappropriate drug identification and failure clinical trials. Thus, solving this doubt is conducive to more appropriate experimental design and data interpretation, and thereby perfecting the drug selection during preclinical phase. The increased investment in preclinical analysis could remarkably promote the effective bench-to-bed translation and largely reduce the rate of attrition of drugs in clinical settings.

In this work, to thoroughly investigate the underlying relationship between cytotoxicity and anticancer efficacy, two kinds of lipid-drug derivatives which utilized ester bond and mono thioether bond to conjugate DTX and linoleic acid (termed DTX-LA and DTX-S-LA) were obtained. Conjugate-induced self-assemble process was used to fabricate nanoassemblies (termed DL NP_S and DSL NP_S). Inhibition abilities were evaluated both in cellular and animal to investigate the *in vitro-in vivo* behaviors. The release behavior, PK and biodistribution study were further investigated.

2. Materials And Methods

2.1 Materials

1,2-distearoyl-sn-glycero-3-phosphoethanolamine-N-[methoxy(polyethyleneglycol)-2000] (DSPE-PEG_{2K}) was purchased from Shanghai Advanced Vehicle Technology Pharmaceutical Co., Ltd. Roswell Park Memorial Institute (RPMI-1640), trypsin, 3-(4, 5-dimethylthiazol-2-yl)-2, 5-diphenyltetrazolium bromide (MTT) and fetal bovine serum (FBS) were purchased from Dalian Meilun Biotechnology Co., Ltd, China. DTX-LA and DTX-S-LA were synthesized and characterized by former work in our lab [12, 29]

2.2 Preparation of DL NPS and DSL NPS

One-step precipitation method was used to prepare the nanoassemblies. In short, 4 mg of DTX-LA or DTX-S-LA and 20% (w/w) DSPE-PEG_{2K} were accurately weighed and dissolved in 100 μL ethanol. Then this miscible solvent containing formulation components was cautiously added dropwise into 2 mL deionized water and continuously stirred for 2 minutes (800 rpm, K-MSH-Pro-6A, JKI, Shanghai, China). Apply vacuum-rotary evaporation procedure for almost 10 min to remove ethanol. Finally, volume with deionized water to 2 mL. Particle size and polydispersity index (PDI) of conjugate NP_S were measured by a Zetasizer (Nano ZS, Malvern, UK) in triplicate.

2.3 Cell lines and cell culture

The murine breast cancer cell line (4T1) was bought from the cell bank of Chinese Academy of Medical Sciences (Beijing, China). 4T1 cells were cultured in RPMI-1640 medium supplemented with 10% FBS,

penicillin (30 mg/L) and streptomycin (100 mg/L) in a humid atmosphere containing 5% CO_2 at 37°C.

2.4 *In vitro* cell viability assay

To explore whether conjugate NP_S could effectively inhibit tumor cells' growth *in vitro*, and more importantly, to provide guidance for *in vivo* experiments, MTT assay was performed in 4T1 cells. A certain density of 4T1 cells (1000 cells/100 μL/well) were incubated in 96 well plates for 12 h to allow cell attachment. Then fresh medium containing a series of concentrations of DTX solution, DL NP_S and DSL NP_S was added to each well to replace old RPMI-1640 medium. Cultivated for another 48 h or 72 h, the drug-contained medium was replaced by 100 μL fresh medium and 20 μL MTT solutions (5 mg/mL) which would be discarded after incubating for 4 h. 200 μL DMSO was added to each well to dissolve the formazan. The absorbance value of each hole in 96 well plates at 570 nm was selected for measurement on a microplate reader (Model500, USA). The Eq. 1 was utilized to calculate the inhibition rate. And the half maximal inhibitory concentrations (IC_{50}) was evaluated by nonlinear regression analysis.

Equation 1: inhibition rate (%) = (1-Asample/Acontrol) × 100

2.5 Animal study

The BALB/c mice and SD rats in this study were offered by the Laboratory Animal Center of Shenyang Pharmaceutical University. All the animal experiments were performed in compliance with the Guide for Care and Use of Laboratory Animals which were approved by the Institutional Animal Ethical Care Committee (IAEC) of Shenyang Pharmaceutical University.

2.6 *In vivo* antitumor efficacy study

To further explore whether these conjugate nanoassemblies could improve the therapeutic index of DTX *in vivo*, anticancer efficacy study should be performed. This study was performed in the female BALB/c mice weighed 18–22 g. In short, the 4T1 cells, suspended in PBS (5×10^6 cells per mouse), were subcutaneously injected into the right auxiliary flank of mice to build tumor-bearing mice models. The mice were divided evenly into 4 groups (n = 5) when the tumor volumes reached almost 120–150 mm^3. Then each group of mice were subjected to treat every two days with saline, Home-made Taxotere (10 mg/kg), DL NP_S (10 mg/kg, DTX equivalence), and DSL NP_S (10 mg/kg, DTX equivalence) via tail vein injection, respectively. The tumor volumes and body weights were monitored and recorded every two days. Tumor volumes were calculated by Eq. 2. After 4 times administration followed by 2 days observation, the mice were sacrificed to collect its' tumors and calculate the tumor burden after the last treatment by Eq. 3.

Equation 2: V (mm^3) = (a^2 × b)/2 (a represents the shortest width and b represents the longest length)

Equation 3: B (%) = w / W × 100% (B represents the tumor burden, w represents the tumor weight and W represents the body weight)

2.7 Physical stability and drug release behavior studies

The physical stability of nanoassemblies was carried out at 4°C for 3 months. The particle size and PDI were determined on a specific time point to monitor the variations. The drug release behavior of DL NP_S and DSL NP_S was performed in plasma. Briefly, the certain concentration of NP_S solution was incubated with mice plasma in an air bath (CHA-S, Guohua Electric Applance Co., Ltd. Jiangsu, China) with the shaking of 100 rpm at 37°C. Plasma samples, at pre-determined time interval, were withdrawn and extracted by acetonitrile for the sedimentation of protein. The supernatant was assessed periodically by HPLC assay on a reverse ODS Cosmosil-C18 column (150 mm × 4.6 mm, 5 μm) with acetonitrile/water (55:45, v/v) for DTX detection and acetonitrile/water (90:10, v/v) for DTX-LA and DTX-S-LA detection. The flow rate was 1.0 mL/min and the detection wavelength was 230 nm.

2.8 Pharmacokinetic properties study

The pharmacokinetic (PK) experiment was carried out on Sprague–Dawley (SD) rats weighed 200–220 g which were divided into 3 groups (n = 5). Administrated with a single intravenous injection of Home-made Taxotere, DL NP_S and DSL NP_S to deliver a DTX equivalent dose of 5 mg/kg, blood samples were withdrawn at pre-determined time intervals via orbital venous plexus. The plasma was collected by centrifugation at 13,000 rpm for 10 min. Precipitation of protein method was applied to extract the drugs. The quantitative analysis was assessed by HPLC-MS/MS with C18 column (100 mm × 2.1 mm, 5 μm). Acetonitrile/water (95:5, v/v) as mobile phase at 0.2 mL/min was used to analyze DTX-LA and DTX-S-LA. The concentration of DTX was determined by elution: 0-0.5 min, 70% water; 0.51–2.5, 5% water; 2.6-3.0, 70% water.

2.9 Bio-distribution study

BALB/c mice bearing 4T1 malignant tumor were used to fulfill biodistribution study. The mice model was built according to antitumor efficacy study's method. The mice were randomly divided into 3 groups (n = 6) and treated with Home-made Taxotere (10 mg/kg), DL NP_S (10 mg/kg, DTX equivalence) and DSL NP_S (10 mg/kg, DTX equivalence) via tail vein injection, respectively. After four and twenty-four hours postinjection, three mice of each group were sacrificed to harvest major organs (heart, liver, spleen, lung and kidney) and tumors. Then the free DTX in tissue homogenate were quantified by HPLC-MS/MS on an ACQUITY UPLC system (Waters Corp). The methods of sample extraction and quantification were in accordance with that of PK study as mentioned above.

3. Results

3.1 Preparation of conjugate NP_S

One-step precipitation method was used to prepare the nanoassemblies (Scheme 1). The particle size confirmed the feasibility of self-assembled nanoparticles. As predicated, once these highly hydrophobic derivatives added to water, self-assemble process would occur to yield an ordered nanoprecipitation. As shown in Fig. 1, the average diameter of DL NP_S and DSL NP_S were both about 100 nm and the PDI was always below 0.2. The DL NP_S and DSL NP_S had spherical shapes with a uniform size of 100 nm.

3.2 *In vitro* cell viability assay

DTX solution, DL NP_S and DSL NP_S were examined against 4T1 cell lines to determine the cytotoxicity. As shown in Fig. 2, more cancerous cells were inhibited as the incubation time prolonged from 48 h to 72 h suggesting the conjugate NP_S had time-dependent inhibition capacity. This could be attributed to that more exposure time was needed to release the active parent drug. Notably, DL NP_S displayed the lowest toxicity against the 4T1 cell lines. The IC_{50} of DSL NP_S and DL NP_S at 48 h were 4.02 and 209.6 ng/mL, respectively.

3.3 *In vivo* antitumor efficacy study

Anticancer ability study was conducted in 4T1 tumor bearing mice. The BALB/c mice were treated with Home-made Taxotere, DL NP_S and DSL NP_S every two days (Fig. 3 (A)). Taxotere is the commercial formulation of DTX which utilized Tween 80 and 13% (w/w, ethanol/water) solution of ethanol as solvents. Surprisingly, despite of 50 folds difference of cytotoxicity, the tumor volumes of DL NP_S group were even smaller than that of DSL NP_S at the same dose level (10 mg/kg, DTX equivalence). After the last treatment, the average tumor volumes of, Home-made Taxotere,DL NP_S and DSL NP_S groups were about 338 ± 65, 245 ± 42 and 329 ± 41 mm^3, respectively. There was an extremely significant difference between saline group and DL NP_S group (Fig. 3 (B)). Besides, as shown in the Fig. 3 (C), the last four days witnessed a notable side effects in the group of Home-made Taxotere with the body weight slumped about 7.8% whereas that of the conjugate NP_S groups maintained the same level off at 20 g. The tumor burden after the last treatment of Home-made Taxotere, DL NP_S and DSL NP_S were about 0.98%, 0.44% and 0.77%, respectively (Fig. 3 (D)). All considered, the outcomes of DL NP_S far exceeded any expectations.

Sum up, compared with DSL NP_S, an unexpected more effective inhibition ability was found in DL NP_S group despite of weaker cytotoxicity *in vitro*. What caused the non-positive correlation? Was cytotoxicity still predictive for efficacy? To figure out these questions, release profiles, PK and bio-distribution studies were further researched in this work.

3.4 Physical stability and drug release behavior studies

DL NP_S and DSL NP_S as potential high drug loading nanotherapeutics, maintaining the integrity of preparation and molecular structure were the prerequisites for them to have a strong anticancer efficacy. Thus, to explore the reasons of non-positive correlation between cytotoxicity and anticancer efficacy, it was a must to study the stability of conjugate nanoparticles. As shown in the physical stability curve (Fig. 4), there were no any significant variations in particle size and PDI implying conjugate NP_S could remain considerably stable within three months in deionized water at 4°C. To further explore the release behavior under more physiological conditions, the conjugate nanoassemblies were placed in plasma samples at 37°C with continuously shaking. Figure 5 (A) illustrated that more than 80% DTX-S-LA conjugates were hydrolyzed within 24 h in plasma, whereas only about 30% DTX-LA degraded in the

same medium. Additionally, less than 5% DTX was converted from DTX-LA conjugates. Based on the values, it was clear that DL NP_S had significantly slower release behavior than DSL NP_S when incubated with blood samples (Fig. 5 (B)). This different release behavior might ascribe to the mono thiother bond inserted conjugates were more susceptible to hydrolysis leading to less stability than ester linked conjugates [30].

3.5 Pharmacokinetic properties study

Derivatives and preparation strategies would dramatically alter the PK profiles in circulation. PK parameters could be suitable values to explore the internal metabolism and provide useful information and reference for explaining the raised questions. The PK study was carried out on SD rats. As shown in the drug concentration-time curve (Fig. 6) and Table 1, the PK profiles could be largely improved by conjugate NP_S. The $t_{1/2}$ of Home-made Taxotere, DTX-LA of DL NP_S and DTX-S-LA of DSL NP_S were 3.21, 4.03 and 4.01 h, respectively. The $t_{1/2}$ had been enlarged 1.3 times by lipid-drug derivative nanoparticles. Remarkably, the AUC of DL NP_S (DTX-LA) even achieved 2 times higher than that of DSL NP_S (DTX-S-LA). This value was crucial important because the pharmacokinetics had a tremendous impact on drug exposure in tumors. Notably, it was not surprising that the proportion of DTX derived from DL NP_S was considerably less than that of DSL NP_S, and this phenomenon was consistent with the results of drug release experiment. The more unstable structure of DTX-S-LA might be the reason that caused the premature DTX release from vesicle in circulation.

Apart from that, the AUC of DTX derived from DSL NP_S was 3 times higher than that of Home-made Taxotere, but higher AUC didn't always mean better anticancer efficacy. Actually there was no difference in anticancer efficacy between DSL NP_S and Home-made Taxotere. This might partly due to the type of surfactant composition. Herein, the concentration of DTX measured contained the unencapsulated drug form fraction and encapsulated form fraction; and the unencapsulated drug form also contained free drug form and plasma protein bonded form. It should be kept in mind that only free form of DTX was bioactive. However, it was very difficult to distinguish from one another because the three forms are in dynamic equilibrium. Besides, some reports clarified that the surfactants were biologically and pharmacologically active and thereby indeed had an influence on the PK profiles or cell uptake [30, 31]. In fact, the administration mode of DTX was different, Home-made Taxotere was a bolus injection, while for DSL NP_S and DL NP_S, the DTX was released from DTX-linoleic acid derivatives at a different rate during the circulation. All above-mentioned reasons complicated the correlation between pharmacokinetic parameters and the efficacy, these need more in depth investigation in the future.

Table 1
Pharmacokinetic parameters of Home-made Taxotere and DTX-linoleic acid nanoassemblies (n = 5 per group).

Formulations	Determined drug	C_{max} (nM/mL)	T_{max} (h)	AUC_{0-12} (nM·h/mL)	$t_{1/2}$ (h)
Home-made Taxotere	DTX	0.71 ± 0.11	0.16 ± 0.11	0.76 ± 0.12	3.21 ± 1.25
DL NP_S	DTX	0.12 ± 0.04	0.23 ± 0.15	0.30 ± 0.07	3.29 ± 1.3
	DTX-LA	81.80 ± 4.44	0.3 ± 0.18	125.6 ± 22.9	4.03 ± 1.1
DSL NP_S	DTX	1.55 ± 0.51	0.32 ± 0.21	2.77 ± 0.88	3.17 ± 0.87
	DTX-S-LA	65.80 ± 21.7	0.21 ± 0.22	64.91 ± 25.43	4.01 ± 1.62

3.6 Bio-distribution study

Considering the biodistribution behavior had an influence on anticancer efficacy and safety profiles, the distribution and bioactivation behavior of conjugate NP_S were investigated in BALB/c mice. The highest DTX concentration in tumor tissues belonged to mice of DL NP_S group (Fig. 7), suggesting DL NP_S could successfully accumulate in tumor sites through passive targeting and get activated by esterases in the tumors. By contrast, the leakage of DSL NP_S in blood circulation was adverse to delivery to the tumor tissues, and the fraction of DTX of DSL NP_S in tumor was significantly less than that of DL NP_S. For Home-made Taxotere, a considerable DTX disposition in spleen and lung was found both at 4 h and 24 h post injection. Fig. 7. Bio-distribution of Home-made Taxotere, DL NP_S and DSL NP_S at 4 h (A) and 24 h (B) postinjection.

4. Discussion

DTX tethered with unsaturated fatty acids had the ability to self-assemble into nanoprecipitations in water. Self-carrier nanoparticles yielded remarkably improved drug loading (61.9% for DL NP_S and 53.4% for DSL NP_S). DSPE-PEG_{2K} as an amphipathic stabilizer could forbid the adsorption of serum proteins enabling NP_S remain stable in bloodstream. Nanostructures without Tween 80 significantly alleviated excipients-induced toxicity with reserving therapeutic efficacy.

Cytotoxic model was a common method for screening anti-tumor agents. Some previous studies also indicated that the lower IC_{50}, the better therapeutic efficacy. But in this work, different results were found. Though inferior cytotoxicity, DL NP_S exhibited unexpected stronger anticancer efficacy when compared

with Home-made Taxotere and DSL NP_S. This non-positive correlation between cytotoxicity *in vitro* and anticancer efficacy *in vivo* could be explained by manifold reasons as below.

The release behavior of conjugate nanoassemblies was performed in plasma sample mediums. The release kinetics revealed that DL NP_S owned much more delayed release behavior suggesting ester bond linked conjugates were considerably more stable than redox sensitive conjugates. That is probably because the mono thioether bond could be easily oxidized to electron-withdrawing sulfone or sulfoxide bearing ROS or esterases, and triggered release [32]. Being stable in extra-cellular environment was important for maintaining the structural integrity. A rapid drug loss was occurred in the group of DSL NP_S when incubated with rat plasma indicating the molecule structure was not stable enough to resist esterases or ROS species in plasma. The relatively unstable structure of DTX-S-LA would reduce the drug exposure in tumor sites. Uncontrolled drug release upon administration would prevent a conjugate candidate from exerting its therapeutic activity. This phenomenon might partly explain the limited antitumor response of DSL NP_S.

The PK study showed that Home-made Taxotere had the shortest $t_{1/2}$ indicating conjugate nanoassemblies could prolong the PK behavior. DL NP_S had the higher AUC (DTX-LA) and less DTX release compared with DSL NP_S which evidenced the ester bond inserted conjugates were more stable in circulation. The phenomenon was consistent with the above release studies *in vitro*. DL NP_S served as a reservoir to inhibit the premature release of parent drug during systemic circulation and thereby would definitely promote the tumor accumulation. And the results of tissue distribution had provided valuable support to this inference.

In conclusion, the relationships between the release profiles, *in vitro* cytotoxicity and *in vivo* antitumor efficacy were of great importance in the lipid-drug selection. The intermediate linker played a vital important role in the results of drug conversion rate. The prodrug-like conjugates should remain structure intact in circulation but get rapid released in tumor sites. Immature release happened in the process of *in vivo* delivery could lead to inadequate drug exposure in tumor sites. In other words, this mono thioether bond linked conjugates were much more vulnerable to hydrolyze than DTX-LA in cytotoxicity assays *in vitro*. Thus, the cell inhibition capacity of DSL NP_S was much stronger in comparison to that of DL NP_S*in vitro*. However, tumor microenvironment was a complex system involving different cellular and non-cellular elements. The cytotoxicity experiments which used growing cells in coated, two-dimensional Petri dishes and glass slides were limited to reproduce the *in vivo* conditions of tumor system. Varied enzymes and lower pH in tumor microenvironment would promote the hydrolysis of ester bonds. Accordingly, more active release could happen in tumor site rather than monotonous adherent cells *in vitro.* Besides, higher AUC and passive target significantly prompted more DL NP_S to accumulate in tumor sites which would certainly contribute to the good anticancer efficacy. However, the MTT assay neglected the circulation process thereby further causing this discrepancy between cytotoxicity and anticancer efficacy.

The *in vivo* disposition was closely interrelated with safety profiles. Poor bio-tolerance was found in the group of Home-made Taxotere with steadfast plunge of body weight. The poor potency of Taxotere to accumulate in tumor sites could explain the off-target toxicity. Compared with the group of Taxotere, the safety of DL NP_S and DSL NP_S had significantly improved. Drastically alleviated toxicity could be explained by the fact that not only excipient-associated side effects had been avoided, but also the tissue distribution behavior had been changed by the NP_S. Additionally, this higher safety profiles further promised a dose escalation for better anticancer efficacy.

5. Conclusions

In this study, two kinds of lipid-drug derivative nanoassemblies had been constructed through the expedient fabrication process. The high drug loading had been considered to be the most notable merits of conjugate NP_S. The nanoassemblies, with very little or no exogenous excipients, provided a possibility to mediate drug delivery in a tumor tissue-specific manner and enhance anticancer effect of prototype. Reduced from potential carriers-induced toxicity, conjugate NP_S had excellent detoxification effect. This nanoplatform for cancer therapy was an invaluable reference for designing more potent drugs for clinical use.

This study would also help researchers increasingly aware that cytotoxic activity was structure-related. For lipid-drug derivatives, no directly positive correlation existed between the cytotoxicity *in vitro* and anticancer efficacy *in vivo*. Even small changes in the structure of drugs or formulations might cause huge alternation behavior *in vivo*. The results of experiments *in vitro* couldn't fully represent or replace *in vivo* experiments. As for the principle of linker design and drug selection, more related studies should be carried out rather than cytotoxicity alone.

Declarations

Ethics approval and consent to participate:

All the animal experiments were performed in compliance with the Guide for Care and Use of Laboratory Animals which were approved by the Institutional Animal Ethical Care Committee (IAEC) of Shenyang Pharmaceutical University.

Consent for publication:

All authors approved the final manuscript and consent for publication.

Availability of data and materials:

https://doi.org/10.7910/DVN/REF6SN

Competing interests:

There are no conflicts of interests to declare.

Funding:

Funding information is not applicable.

Authors' contributions:

Yongjun Wang and Zhonggui He both contributed to the study conception and design. Material preparation, data collection and analysis were performed by Lirui Jia, Ying Liu and Meng Li. The first draft of the manuscript was written by Lirui Jia and all authors commented on previous versions of the manuscript. All authors read and approved the final manuscript.

Acknowledgements:

This work was financially supported by the Career Development Program for Young and Middle-aged Teachers in Shenyang Pharmaceutical University.

References

1. B. Seruga, A. Ocana, I.F. Tannock, Drug resistance in metastatic castration-resistant prostate cancer, Nat Rev Clin Oncol, 8 (2011) 12-23.
2. P.M. Drisya, E. James, Recent updates in the management of chemotherapy induced nausea and vomiting, Asian Journal of Pharmaceutical and Clinical Research, 6 (2013) 5-10.
3. L.M. Colli, M.J. Machiela, H. Zhang, T.A. Myers, L. Jessop, O. Delattre, K. Yu, S.J. Chanock, Landscape of Combination Immunotherapy and Targeted Therapy to Improve Cancer Management, Cancer Res, 77 (2017) 3666-3671.
4. F. Migliorini, J. Eschweiler, A. Trivellas, A. Driessen, M. Knobe, M.T.N. Maffulli, Better pain control with 8-gray single fraction palliative radiotherapy for skeletal metastases_ a Bayesian network meta-analysis, Clinical & Experimental Metastasis, (2020).
5. P. Adhikari, P. Pal, A.K. Das, S. Ray, A. Bhattacharjee, B. Mazumder, Nano lipid-drug conjugate: An integrated review, International Journal of Pharmaceutics, 529 (2017) 629-641.
6. T. Date, K. Paul, N. Singh, S. Jain, Drug–Lipid Conjugates for Enhanced Oral Drug Delivery, AAPS PharmSciTech, 20 (2019).
7. D. Irby, C. Du, F. Li, Lipid–Drug Conjugate for Enhancing Drug Delivery, molecular pharmaceutics, 14 (2017) 1325-1338.
8. N.R. Brownlee, J.J. Huttner, R.V. Panganamala, D.G. Cornwell, Role of vitamin E in glutathione-induced oxidant stress: methemoglobin, lipid peroxidation, and hemolysis, Journal of Lipid Research, 18 (1977) 635-644.
9. M. Gao, X. Meng, X. Guo, J. Zhu, A. Fan, Z. Wang, Y. Zhao, All-active antitumor micelles via triggered lipid peroxidation, Journal of Controlled Release, 286 (2018) 381-393.

10. H. Park, W. Park, K. Na, Doxorubicin loaded singlet-oxygen producible polymeric micelle based on chlorine e6 conjugated pluronic F127 for overcoming drug resistance in cancer, Biomaterials, 35 (2014) 7963-7969.
11. N. Thotakura, M. Dadarwal, P. Kumar, G. Sharma, S.K. Guru, S. Bhushan, K. Raza, O.P. Katare, Chitosan-Stearic Acid Based Polymeric Micelles for the Effective Delivery of Tamoxifen: Cytotoxic and Pharmacokinetic Evaluation, AAPS PharmSciTech, 18 (2017) 759-768.
12. M. Li, L. Zhao, T. Zhang, Yue Shu, Z. He, Y. Ma, D. Liu, Y. Wang, Redox Sensitive Prodrug Nanoassemblies Based on LinoleicAcid Modified Docetaxel, Acta Pharmaceutica Sinica B, 9 (2019) 421-432.
13. C. Luo, J. Sun, D. Liu, B. Sun, L. Miao, S. Musetti, J. Li, X. Han, Y. Du, L. Li, L. Huang, Z. He, Self-Assembled Redox Dual-Responsive Prodrug-Nanosystem Formed by Single Thioether-Bridged Paclitaxel-Fatty Acid Conjugate for Cancer Chemotherapy, Nano Lett, 16 (2016) 5401-5408.
14. B. Sun, C. Luo, H. Yu, X. Zhang, Q. Chen, W. Yang, M. Wang, Q. Kan, H. Zhang, Y. Wang, Z. He, J. Sun, Disulfide Bond-Driven Oxidation- and Reduction-Responsive Prodrug Nanoassemblies for Cancer Therapy, Nano Lett, 18 (2018) 3643-3650.
15. W. Wei, C. Luo, J. Yang, B. Sun, D. Zhao, Y. Liu, Y. Wang, W. Yang, Q. Kan, J. Sun, Z. He, Precisely albumin-hitchhiking tumor cell-activated reduction/oxidation-responsive docetaxel prodrugs for the hyperselective treatment of breast cancer, J Control Release, 285 (2018) 187-199.
16. P. Xue, D. Liu, J. Wang, N. Zhang, J. Zhou, L. Li, W. Guo, M. Sun, X. Han, Y. Wang, Redox-Sensitive Citronellol-Cabazitaxel Conjugate: Maintained in Vitro Cytotoxicity and Self-Assembled as Multifunctional Nanomedicine, Bioconjug Chem, 27 (2016) 1360-1372.
17. S. Zhang, J. Guan, M. Sun, D. Zhang, H. Zhang, B. Sun, W. Guo, B. Lin, Y. Wang, Z. He, C. Luo, J. Sun, Self-delivering prodrug-nanoassemblies fabricated by disulfide bond bridged oleate prodrug of docetaxel for breast cancer therapy, Drug Deliv, 24 (2017) 1460-1469.
18. A. Monks, D. Scudiero, P. Skehan, R. Shoemaker, K. Paull, D. Vistica, C. Hose, J. Langley, P. Cronise, A. Vaigro-Wolff, M. Gray-Goodrich, H. Campbell, J. Mayo, M. Boyd, Feasibility of a High-Flux Anticancer Drug Screen Using a Diverse Panel of Cultured Human Tumor Cell Lines, Journal of the National Cancer Institute, 83 (1991) 757-766.
19. V. Gonzalez-Nicolin, M. Fussenegger, In vitro assays for anticancer drug discovery—a novel approach based on engineered mammalian cell lines, Anti-Cancer Drugs, 15 (2005) 223-228.
20. J.L. Wilding, W.F. Bodmer, Cancer cell lines for drug discovery and development, Cancer Res, 74 (2014) 2377-2384.
21. R.M. Eglen, A. Gilchrist, T. Reisine, The Use of Immortalized Cell Lines in GPCR Screening: The Good, Bad and Ugly, Combinatorial Chemistry & High Throughput Screening, 11 (2008) 560-565.
22. H. Wang, Z. Lu, L. Wang, T. Guo, J. Wu, J. Wan, L. Zhou, H. Li, Z. Li, D. Jiang, P. Song, H. Xie, L. Zhou, X. Xu, S. Zheng, New Generation Nanomedicines Constructed from Self-Assembling Small-Molecule Prodrugs Alleviate Cancer Drug Toxicity, Cancer Res, 77 (2017) 6963-6974.

23. J. Cui, C. Li, W. Guo, Y. Li, C. Wang, L. Zhang, L. Zhang, Y. Hao, Y. Wang, Direct comparison of two pegylated liposomal doxorubicin formulations: is AUC predictive for toxicity and efficacy?, J Control Release, 118 (2007) 204-215.
24. R.D. Signorell, P. Luciani, D. Brambilla, J.C. Leroux, Pharmacokinetics of lipid-drug conjugates loaded into liposomes, Eur J Pharm Biopharm, 128 (2018) 188-199.
25. V. Das, F. Bruzzese, P. Konecny, F. Iannelli, A. Budillon, M. Hajduch, Pathophysiologically relevant in vitro tumor models for drug screening, Drug Discov Today, 20 (2015) 848-855.
26. A. Eastman, Improving anticancer drug development begins with cell culture: misinformation perpetrated by the misuse of cytotoxicity assays, Oncotarget, 8 (2016) 8854-8866.
27. S.M. Ansell, S.A. Johnstone, P.G. Tardi, L. Lo, S. Xie, Y. Shu, T.O. Harasym, N.L. Harasym, L. Williams, D. Bermudes, B.D. Liboiron, W. Saad, R.K. Prud'homme, L.D. Maye, Modulating the Therapeutic Activity of Nanoparticle Delivered Paclitaxel by Manipulating the Hydrophobicity of Prodrug Conjugates, Journal of Medicinal Chemistry 51 (2008).
28. J. Wang, P. Xue, J. Zhou, L. Li, L. Xu, Y. Wang, Comparison of two kinds of docetaxel-vitamin E prodrugs: in vitro evaluation and in vivo antitumor activity, International Journal of Pharmaceutics, 505 (2016) 352-360.
29. T. Zhang, M. Li, R. Yang, D. Zhang, J. Guan, J. Yua, B. Yang, H. Zhang, S. Zhang, D. Liu, Y. Wang, Therapeutic efficacy of lipid emulsions of docetaxel-linoleic acid conjugate in breast cancer, International Journal of Pharmaceutics, 546 (2018) 61-69.
30. E.-H. Lee, S.-S. Hong, S.H. Kim, M.-K. Lee, J.S. Lim, S.-J. Lim, Computed Tomography-Guided Screening of Surfactant Effect on Blood Circulation Time of Emulsions: Application to the Design of an Emulsion Formulation for Paclitaxel, Pharmaceutical research, 31 (2014) 2022-2034.
31. K.L. Hennenfent, R. Govindan, Novel formulations of taxanes: a review. Old wine in a new bottle?, Annals of Oncology, 17 (2005) 735-749.
32. J. Wang, X. Sun, W. Mao, W. Sun, J. Tang, M. Sui, Y. Shen, Z. Gu, Tumor Redox Heterogeneity-Responsive Prodrug Nanocapsules for Cancer Chemotherapy, ADVANCED MATERIALS, 25 (2013) 3670-3676.

Figures

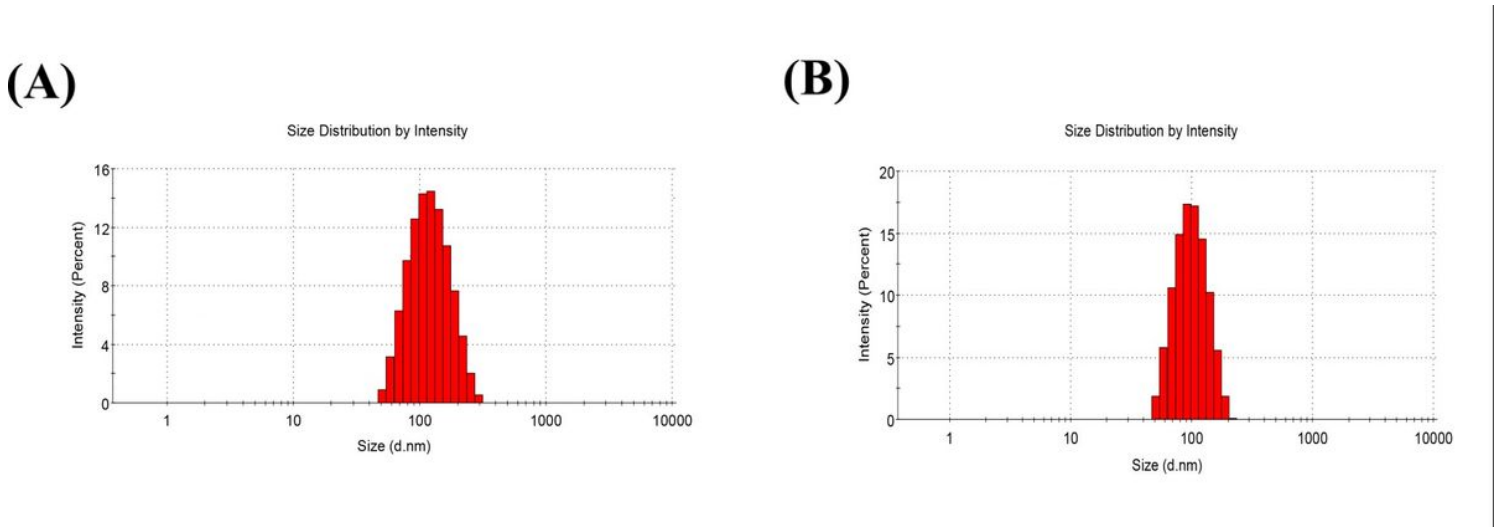

Figure 1

The size diameter of DL NPS (A) and DSL NPS (B) measured by a Zetasizer

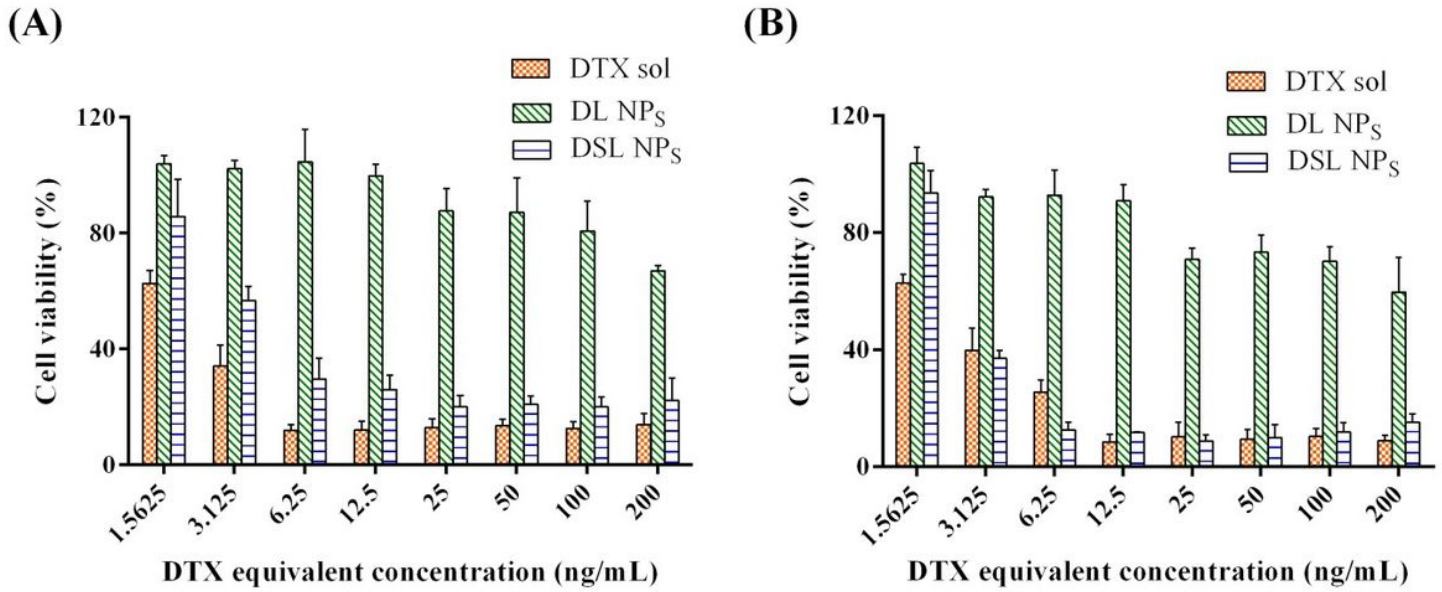

Figure 2

The cell viability at various concentration of conjugate NPS and DTX solution at 48 h (A) and 72 h (B).

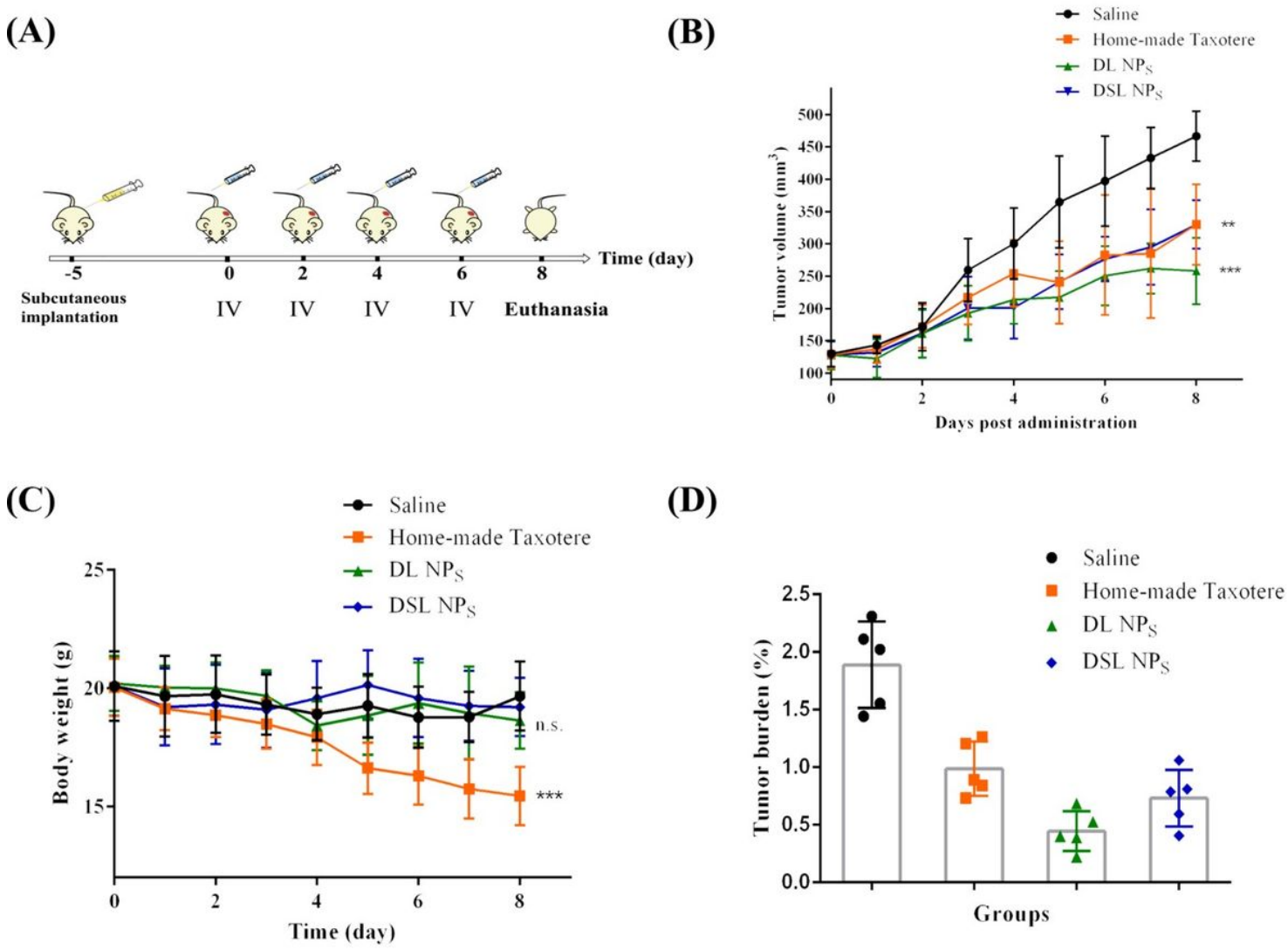

Figure 3

The observation of tumor growth and system safety when treatment with Home-made Taxotere, DL NPS and DSL NPS. (A) Outline the experimental schedule (n = 5); (B) The changes of volumes after various treatment; (C) The body weight-time curve for 4 groups; (D) Tumor burden after the last treatment. ** P < 0.01 and *** P < 0.001 between the groups indicated.

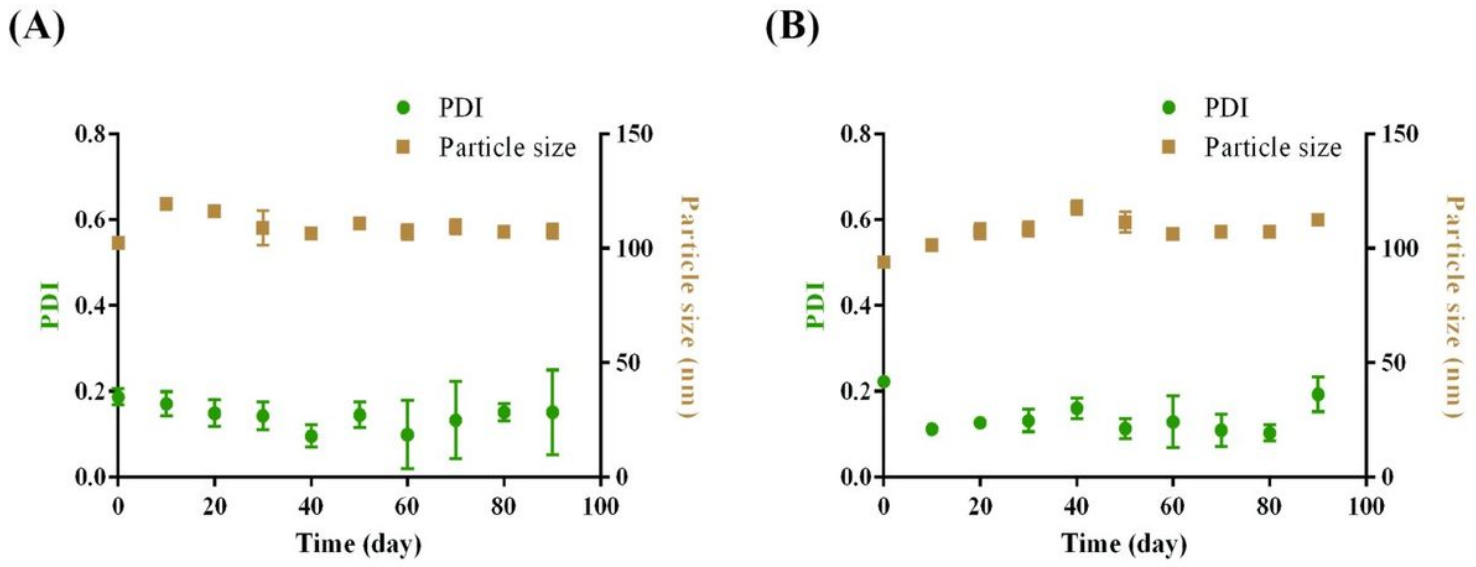

Figure 4

Long term stability of DL NPS and DSL NPS after store at 4°C for 90 d.

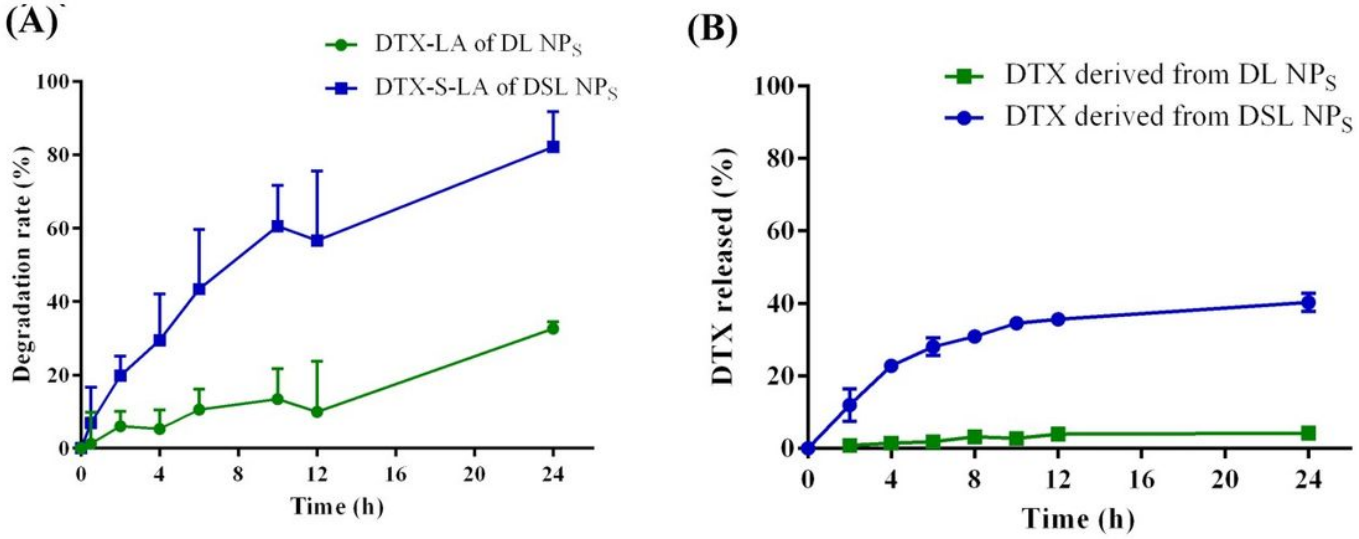

Figure 5

(A) The degradation rate of derivatives NPS when incubated with plasma; (B) Cumulative DTX release from derivative NPS at plasma (n = 3).

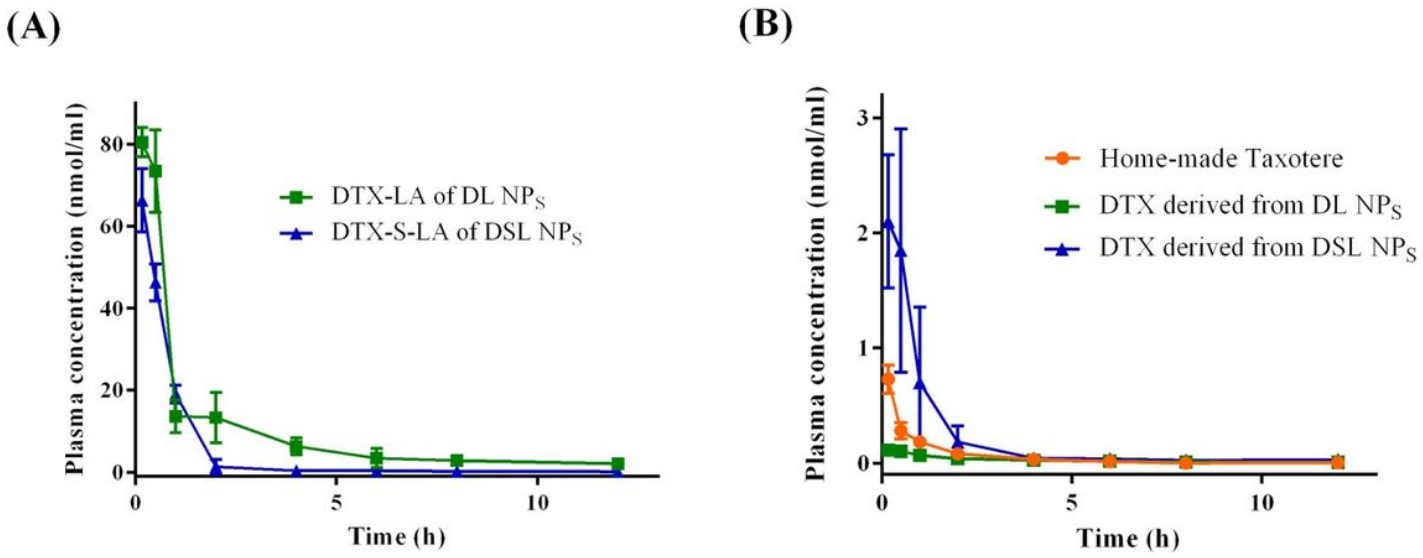

Figure 6

In vivo plasma concentration-time profiles of derivatives (A) and DTX (B) after tail vein injection of Home-made Taxotere, DL NPS and DSL NPS at a DTX equivalent dose of 5mg/kg (n = 5).

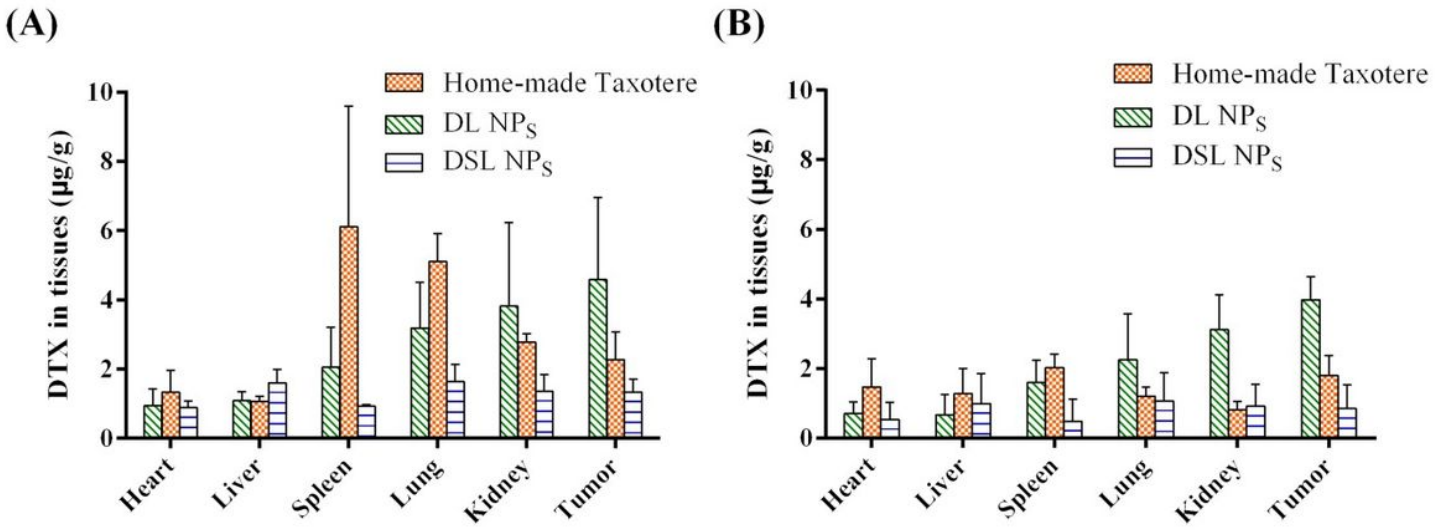

Figure 7

Bio-distribution of Home-made Taxotere, DL NPS and DSL NPS at 4 h (A) and 24 h (B) postinjection.

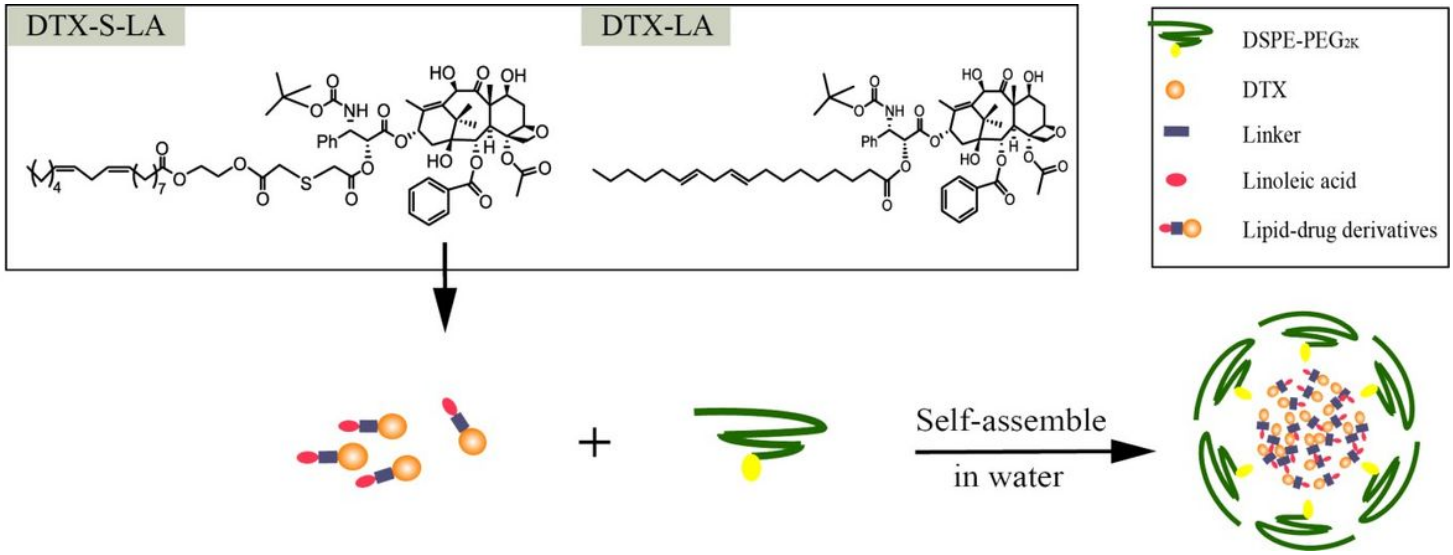

Figure 8

Scheme representation of derivative NPS

Supplementary Files

This is a list of supplementary files associated with this preprint. Click to download.

- GraphicalAbstract.jpg